University of Nebraska - Lincoln
DigitalCommons@University of Nebraska - Lincoln

Kenneth Bloom Publications | Research Papers in Physics and Astronomy

1-1-2012

Measurement of the relative branching ratio of B0s→ J/ΨΦ(980) to B0s→ J/ΨΦ

V. M. Abazov
Joint Institute for Nuclear Research, Dubna, Russia

Kenneth A. Bloom
University of Nebraska - Lincoln, kbloom2@unl.edu

Daniel R. Claes
University of Nebraska - Lincoln, dclaes1@unl.edu

Kayle DeVaughan
University of Nebraska-Lincoln

A. Dominguez
University of Nebraska - Lincoln, adominguez2@unl.edu

See next page for additional authors

Follow this and additional works at: http://digitalcommons.unl.edu/physicsbloom

Part of the Physics Commons

Abazov, V. M.; Bloom, Kenneth A.; Claes, Daniel R.; DeVaughan, Kayle; Dominguez, A.; Eads, Michael; Katsanos, Ioannis; Malik, Sudhir; Snow, Gregory; and D0 Collaboration, "Measurement of the relative branching ratio of B0s→ J/ΨΦ(980) to B0s→ J/ΨΦ" (2012). *Kenneth Bloom Publications.* Paper 323.
http://digitalcommons.unl.edu/physicsbloom/323

This Article is brought to you for free and open access by the Research Papers in Physics and Astronomy at DigitalCommons@University of Nebraska - Lincoln. It has been accepted for inclusion in Kenneth Bloom Publications by an authorized administrator of DigitalCommons@University of Nebraska - Lincoln.

Authors
V. M. Abazov, Kenneth A. Bloom, Daniel R. Claes, Kayle DeVaughan, A. Dominguez, Michael Eads, Ioannis Katsanos, Sudhir Malik, Gregory Snow, and D0 Collaboration

This article is available at DigitalCommons@University of Nebraska - Lincoln: http://digitalcommons.unl.edu/physicsbloom/323

PHYSICAL REVIEW D **85,** 011103(R) (2012)

Measurement of the relative branching ratio of $B_s^0 \to J/\psi f_0(980)$ to $B_s^0 \to J/\psi \phi$

V. M. Abazov,[34] B. Abbott,[72] B. S. Acharya,[28] M. Adams,[48] T. Adams,[46] G. D. Alexeev,[34] G. Alkhazov,[38] A. Alton,[60,*] G. Alverson,[59] G. A. Alves,[2] M. Aoki,[47] A. Askew,[46] B. Åsman,[40] S. Atkins,[57] O. Atramentov,[64] K. Augsten,[9] C. Avila,[7] J. BackusMayes,[79] F. Badaud,[12] L. Bagby,[47] B. Baldin,[47] D. V. Bandurin,[46] S. Banerjee,[28] E. Barberis,[59] P. Baringer,[55] J. Barreto,[3] J. F. Bartlett,[47] U. Bassler,[17] V. Bazterra,[48] A. Bean,[55] M. Begalli,[3] C. Belanger-Champagne,[40] L. Bellantoni,[47] S. B. Beri,[26] G. Bernardi,[16] R. Bernhard,[21] I. Bertram,[41] M. Besançon,[17] R. Beuselinck,[42] V. A. Bezzubov,[37] P. C. Bhat,[47] V. Bhatnagar,[26] G. Blazey,[49] S. Blessing,[46] K. Bloom,[63] A. Boehnlein,[47] D. Boline,[69] E. E. Boos,[36] G. Borissov,[41] T. Bose,[58] A. Brandt,[75] O. Brandt,[22] R. Brock,[61] G. Brooijmans,[67] A. Bross,[47] D. Brown,[16] J. Brown,[16] X. B. Bu,[47] M. Buehler,[47] V. Buescher,[23] V. Bunichev,[36] S. Burdin,[41,†] T. H. Burnett,[79] C. P. Buszello,[40] B. Calpas,[14] E. Camacho-Pérez,[31] M. A. Carrasco-Lizarraga,[55] B. C. K. Casey,[47] H. Castilla-Valdez,[31] S. Chakrabarti,[69] D. Chakraborty,[49] K. M. Chan,[53] A. Chandra,[77] E. Chapon,[17] G. Chen,[55] S. Chevalier-Théry,[17] D. K. Cho,[74] S. W. Cho,[30] S. Choi,[30] B. Choudhary,[27] S. Cihangir,[47] D. Claes,[63] J. Clutter,[55] M. Cooke,[47] W. E. Cooper,[47] M. Corcoran,[77] F. Couderc,[17] M.-C. Cousinou,[14] A. Croc,[17] D. Cutts,[74] A. Das,[44] G. Davies,[42] K. De,[75] S. J. de Jong,[33] E. De La Cruz-Burelo,[31] F. Déliot,[17] R. Demina,[68] D. Denisov,[47] S. P. Denisov,[37] S. Desai,[47] C. Deterre,[17] K. DeVaughan,[63] H. T. Diehl,[47] M. Diesburg,[47] P. F. Ding,[43] A. Dominguez,[63] T. Dorland,[79] A. Dubey,[27] L. V. Dudko,[36] D. Duggan,[64] A. Duperrin,[14] S. Dutt,[26] A. Dyshkant,[49] M. Eads,[63] D. Edmunds,[61] J. Ellison,[45] V. D. Elvira,[47] Y. Enari,[16] H. Evans,[51] A. Evdokimov,[70] V. N. Evdokimov,[37] G. Facini,[59] T. Ferbel,[68] F. Fiedler,[23] F. Filthaut,[33] W. Fisher,[61] H. E. Fisk,[47] M. Fortner,[49] H. Fox,[41] S. Fuess,[47] A. Garcia-Bellido,[68] G. A García-Guerra,[31,‡] V. Gavrilov,[35] P. Gay,[12] W. Geng,[14,61] D. Gerbaudo,[65] C. E. Gerber,[48] Y. Gershtein,[64] G. Ginther,[47,68] G. Golovanov,[34] A. Goussiou,[79] P. D. Grannis,[69] S. Greder,[18] H. Greenlee,[47] Z. D. Greenwood,[57] E. M. Gregores,[4] G. Grenier,[19] Ph. Gris,[12] J.-F. Grivaz,[15] A. Grohsjean,[17] S. Grünendahl,[47] M. W. Grünewald,[29] T. Guillemin,[15] G. Gutierrez,[47] P. Gutierrez,[72] A. Haas,[67,§] S. Hagopian,[46] J. Haley,[59] L. Han,[6] K. Harder,[43] A. Harel,[68] J. M. Hauptman,[54] J. Hays,[42] T. Head,[43] T. Hebbeker,[20] D. Hedin,[49] H. Hegab,[73] A. P. Heinson,[45] U. Heintz,[74] C. Hensel,[22] I. Heredia-De La Cruz,[31] K. Herner,[60] G. Hesketh,[43,‖] M. D. Hildreth,[53] R. Hirosky,[78] T. Hoang,[46] J. D. Hobbs,[69] B. Hoeneisen,[11] M. Hohlfeld,[23] Z. Hubacek,[9,17] V. Hynek,[9] I. Iashvili,[66] Y. Ilchenko,[76] R. Illingworth,[47] A. S. Ito,[47] S. Jabeen,[74] M. Jaffré,[15] D. Jamin,[14] A. Jayasinghe,[72] R. Jesik,[42] K. Johns,[44] M. Johnson,[47] A. Jonckheere,[47] P. Jonsson,[42] J. Joshi,[26] A. W. Jung,[47] A. Juste,[39] K. Kaadze,[56] E. Kajfasz,[14] D. Karmanov,[36] P. A. Kasper,[47] I. Katsanos,[63] R. Kehoe,[76] S. Kermiche,[14] N. Khalatyan,[47] A. Khanov,[73] A. Kharchilava,[66] Y. N. Kharzheev,[34] J. M. Kohli,[26] A. V. Kozelov,[37] J. Kraus,[61] S. Kulikov,[37] A. Kumar,[66] A. Kupco,[10] T. Kurča,[19] V. A. Kuzmin,[36] J. Kvita,[8] S. Lammers,[51] G. Landsberg,[74] P. Lebrun,[19] H. S. Lee,[30] S. W. Lee,[54] W. M. Lee,[47] J. Lellouch,[16] L. Li,[45] Q. Z. Li,[47] S. M. Lietti,[5] J. K. Lim,[30] D. Lincoln,[47] J. Linnemann,[61] V. V. Lipaev,[37] R. Lipton,[47] Y. Liu,[6] A. Lobodenko,[38] M. Lokajicek,[10] R. Lopes de Sa,[69] H. J. Lubatti,[79] R. Luna-Garcia,[31,¶] A. L. Lyon,[47] A. K. A. Maciel,[2] D. Mackin,[77] R. Madar,[17] R. Magaña-Villalba,[31] S. Malik,[63] V. L. Malyshev,[34] Y. Maravin,[56] J. Martínez-Ortega,[31] R. McCarthy,[69] C. L. McGivern,[55] M. M. Meijer,[33] A. Melnitchouk,[62] D. Menezes,[49] P. G. Mercadante,[4] M. Merkin,[36] A. Meyer,[20] J. Meyer,[22] F. Miconi,[18] N. K. Mondal,[28] G. S. Muanza,[14] M. Mulhearn,[78] E. Nagy,[14] M. Naimuddin,[27] M. Narain,[74] R. Nayyar,[27] H. A. Neal,[60] J. P. Negret,[7] P. Neustroev,[38] S. F. Novaes,[5] T. Nunnemann,[24] G. Obrant,[38,‡‡] J. Orduna,[77] N. Osman,[14] J. Osta,[53] G. J. Otero y Garzón,[1] M. Padilla,[45] A. Pal,[75] N. Parashar,[52] V. Parihar,[74] S. K. Park,[30] R. Partridge,[74,§] N. Parua,[51] A. Patwa,[70] B. Penning,[47] M. Perfilov,[36] Y. Peters,[43] K. Petridis,[43] G. Petrillo,[68] P. Pétroff,[15] R. Piegaia,[1] M.-A. Pleier,[70] P. L. M. Podesta-Lerma,[31,**] V. M. Podstavkov,[47] P. Polozov,[35] A. V. Popov,[37] M. Prewitt,[77] D. Price,[51] N. Prokopenko,[37] J. Qian,[60] A. Quadt,[22] B. Quinn,[62] M. S. Rangel,[2] K. Ranjan,[27] P. N. Ratoff,[41] I. Razumov,[37] P. Renkel,[76] M. Rijssenbeek,[69] I. Ripp-Baudot,[18] F. Rizatdinova,[73] M. Rominsky,[47] A. Ross,[41] C. Royon,[17] P. Rubinov,[47] R. Ruchti,[53] G. Safronov,[35] G. Sajot,[13] P. Salcido,[49] A. Sánchez-Hernández,[31] M. P. Sanders,[24] B. Sanghi,[47] A. S. Santos,[5] G. Savage,[47] L. Sawyer,[57] T. Scanlon,[42] R. D. Schamberger,[69] Y. Scheglov,[38] H. Schellman,[50] T. Schliephake,[25] S. Schlobohm,[79] C. Schwanenberger,[43] R. Schwienhorst,[61] J. Sekaric,[55] H. Severini,[72] E. Shabalina,[22] V. Shary,[17] A. A. Shchukin,[37] R. K. Shivpuri,[27] V. Simak,[9] V. Sirotenko,[47] P. Skubic,[72] P. Slattery,[68] D. Smirnov,[53] K. J. Smith,[66] G. R. Snow,[63] J. Snow,[71] S. Snyder,[70] S. Söldner-Rembold,[43] L. Sonnenschein,[20] K. Soustruznik,[8] J. Stark,[13] V. Stolin,[35] D. A. Stoyanova,[37] M. Strauss,[72] D. Strom,[48] L. Stutte,[47] L. Suter,[43] P. Svoisky,[72] M. Takahashi,[43] A. Tanasijczuk,[1] M. Titov,[17] V. V. Tokmenin,[34] Y.-T. Tsai,[68] K. Tschann-Grimm,[69] D. Tsybychev,[69] B. Tuchming,[17] C. Tully,[65] L. Uvarov,[38] S. Uvarov,[38] S. Uzunyan,[49] R. Van Kooten,[51] W. M. van Leeuwen,[32] N. Varelas,[48] E. W. Varnes,[44] I. A. Vasilyev,[37] P. Verdier,[19] L. S. Vertogradov,[34] M. Verzocchi,[47] M. Vesterinen,[43] D. Vilanova,[17] P. Vokac,[9] H. D. Wahl,[46] M. H. L. S. Wang,[47] J. Warchol,[53] G. Watts,[79] M. Wayne,[53] M. Weber,[47,††] L. Welty-Rieger,[50] A. White,[75] D. Wicke,[25]

 © 2012 American Physical Society

M. R. J. Williams,[41] G. W. Wilson,[55] M. Wobisch,[57] D. R. Wood,[59] T. R. Wyatt,[43] Y. Xie,[47] R. Yamada,[47] W.-C. Yang,[43] T. Yasuda,[47] Y. A. Yatsunenko,[34] Z. Ye,[47] H. Yin,[47] K. Yip,[70] S. W. Youn,[47] J. Yu,[75] T. Zhao,[79] B. Zhou,[60] J. Zhu,[60] M. Zielinski,[68] D. Zieminska,[51] and L. Zivkovic[74]

(The D0 Collaboration)

[1]*Universidad de Buenos Aires, Buenos Aires, Argentina*
[2]*LAFEX, Centro Brasileiro de Pesquisas Físicas, Rio de Janeiro, Brazil*
[3]*Universidade do Estado do Rio de Janeiro, Rio de Janeiro, Brazil*
[4]*Universidade Federal do ABC, Santo André, Brazil*
[5]*Instituto de Física Teórica, Universidade Estadual Paulista, São Paulo, Brazil*
[6]*University of Science and Technology of China, Hefei, People's Republic of China*
[7]*Universidad de los Andes, Bogotá, Colombia*
[8]*Charles University, Faculty of Mathematics and Physics, Center for Particle Physics, Prague, Czech Republic*
[9]*Czech Technical University in Prague, Prague, Czech Republic*
[10]*Center for Particle Physics, Institute of Physics, Academy of Sciences of the Czech Republic, Prague, Czech Republic*
[11]*Universidad San Francisco de Quito, Quito, Ecuador*
[12]*LPC, Université Blaise Pascal, CNRS/IN2P3, Clermont, France*
[13]*LPSC, Université Joseph Fourier Grenoble 1, CNRS/IN2P3, Institut National Polytechnique de Grenoble, Grenoble, France*
[14]*CPPM, Aix-Marseille Université, CNRS/IN2P3, Marseille, France*
[15]*LAL, Université Paris-Sud, CNRS/IN2P3, Orsay, France*
[16]*LPNHE, Universités Paris VI and VII, CNRS/IN2P3, Paris, France*
[17]*CEA, Irfu, SPP, Saclay, France*
[18]*IPHC, Université de Strasbourg, CNRS/IN2P3, Strasbourg, France*
[19]*IPNL, Université Lyon 1, CNRS/IN2P3, Villeurbanne, France and Université de Lyon, Lyon, France*
[20]*III. Physikalisches Institut A, RWTH Aachen University, Aachen, Germany*
[21]*Physikalisches Institut, Universität Freiburg, Freiburg, Germany*
[22]*II. Physikalisches Institut, Georg-August-Universität Göttingen, Göttingen, Germany*
[23]*Institut für Physik, Universität Mainz, Mainz, Germany*
[24]*Ludwig-Maximilians-Universität München, München, Germany*
[25]*Fachbereich Physik, Bergische Universität Wuppertal, Wuppertal, Germany*
[26]*Panjab University, Chandigarh, India*
[27]*Delhi University, Delhi, India*
[28]*Tata Institute of Fundamental Research, Mumbai, India*
[29]*University College Dublin, Dublin, Ireland*
[30]*Korea Detector Laboratory, Korea University, Seoul, Korea*
[31]*CINVESTAV, Mexico City, Mexico*
[32]*Nikhef, Science Park, Amsterdam, the Netherlands*
[33]*Radboud University Nijmegen, Nijmegen, the Netherlands and Nikhef, Science Park, Amsterdam, the Netherlands*
[34]*Joint Institute for Nuclear Research, Dubna, Russia*
[35]*Institute for Theoretical and Experimental Physics, Moscow, Russia*
[36]*Moscow State University, Moscow, Russia*
[37]*Institute for High Energy Physics, Protvino, Russia*
[38]*Petersburg Nuclear Physics Institute, St. Petersburg, Russia*
[39]*Institució Catalana de Recerca i Estudis Avançats (ICREA) and Institut de Física d'Altes Energies (IFAE), Barcelona, Spain*
[40]*Stockholm University, Stockholm and Uppsala University, Uppsala, Sweden*
[41]*Lancaster University, Lancaster LA1 4YB, United Kingdom*
[42]*Imperial College London, London SW7 2AZ, United Kingdom*
[43]*The University of Manchester, Manchester M13 9PL, United Kingdom*
[44]*University of Arizona, Tucson, Arizona 85721, USA*
[45]*University of California Riverside, Riverside, California 92521, USA*
[46]*Florida State University, Tallahassee, Florida 32306, USA*
[47]*Fermi National Accelerator Laboratory, Batavia, Illinois 60510, USA*
[48]*University of Illinois at Chicago, Chicago, Illinois 60607, USA*
[49]*Northern Illinois University, DeKalb, Illinois 60115, USA*
[50]*Northwestern University, Evanston, Illinois 60208, USA*
[51]*Indiana University, Bloomington, Indiana 47405, USA*
[52]*Purdue University Calumet, Hammond, Indiana 46323, USA*
[53]*University of Notre Dame, Notre Dame, Indiana 46556, USA*

[54]*Iowa State University, Ames, Iowa 50011, USA*
[55]*University of Kansas, Lawrence, Kansas 66045, USA*
[56]*Kansas State University, Manhattan, Kansas 66506, USA*
[57]*Louisiana Tech University, Ruston, Louisiana 71272, USA*
[58]*Boston University, Boston, Massachusetts 02215, USA*
[59]*Northeastern University, Boston, Massachusetts 02115, USA*
[60]*University of Michigan, Ann Arbor, Michigan 48109, USA*
[61]*Michigan State University, East Lansing, Michigan 48824, USA*
[62]*University of Mississippi, University, Mississippi 38677, USA*
[63]*University of Nebraska, Lincoln, Nebraska 68588, USA*
[64]*Rutgers University, Piscataway, New Jersey 08855, USA*
[65]*Princeton University, Princeton, New Jersey 08544, USA*
[66]*State University of New York, Buffalo, New York 14260, USA*
[67]*Columbia University, New York, New York 10027, USA*
[68]*University of Rochester, Rochester, New York 14627, USA*
[69]*State University of New York, Stony Brook, New York 11794, USA*
[70]*Brookhaven National Laboratory, Upton, New York 11973, USA*
[71]*Langston University, Langston, Oklahoma 73050, USA*
[72]*University of Oklahoma, Norman, Oklahoma 73019, USA*
[73]*Oklahoma State University, Stillwater, Oklahoma 74078, USA*
[74]*Brown University, Providence, Rhode Island 02912, USA*
[75]*University of Texas, Arlington, Texas 76019, USA*
[76]*Southern Methodist University, Dallas, Texas 75275, USA*
[77]*Rice University, Houston, Texas 77005, USA*
[78]*University of Virginia, Charlottesville, Virginia 22901, USA*
[79]*University of Washington, Seattle, Washington 98195, USA*
(Received 20 October 2011; published 20 January 2012)

We present a measurement of the relative branching fraction, $R_{f_0/\phi}$, of $B_s^0 \to J/\psi f_0(980)$, with $f_0(980) \to \pi^+\pi^-$, to the process $B_s^0 \to J/\psi\phi$, with $\phi \to K^+K^-$. The $J/\psi f_0(980)$ final state corresponds to a CP-odd eigenstate of B_s^0 that could be of interest in future studies of CP violation. Using 8 fb^{-1} of data recorded with the D0 detector at the Fermilab Tevatron Collider, we find $R_{f_0/\phi} = 0.275 \pm 0.041(\text{stat}) \pm 0.061(\text{syst})$.

DOI: 10.1103/PhysRevD.85.011103 PACS numbers: 13.25.Hw, 14.40.Nd

The CP-violating phase angle in B_s^0 mixing, $\phi_s^{J/\psi\phi}$, has been measured [1–3] using $B_s^0 \to J/\psi\phi$ decays, and is statistically consistent with that predicted by the standard model (SM) [4]. Ignoring possible ambiguities in its hadronic structure [5], the weak phase angle $\phi_s^{c\bar{c}s\bar{s}}$ measured in $B_s^0 \to J/\psi f_0(980)$ decay should be equal to the angle $\phi_s^{J/\psi\phi} = -2\beta_s^{\text{SM}} + \phi_s^{\text{NP}}$, where β_s^{SM} is the SM angle in the unitarity triangle for the B_s^0 system that is analogous to the well-known angle β in the B_d^0 system, and ϕ_s^{NP} is any additional phase arising from new physics in B_s^0 mixing. Measuring this phase angle through various decay modes could help reduce its uncertainty. In particular, the decay products of $B_s^0 \to J/\psi\phi$ are in an indefinite CP state, requiring CP-even and CP-odd components to be extracted through a time-dependent angular analysis. In contrast, the decay products in $B_s^0 \to J/\psi f_0(980)$ are in a CP-odd eigenstate, which can provide a more direct measurement of $\phi_s^{c\bar{c}s\bar{s}}$ relative to $B_s^0 \to J/\psi\phi$ [6]. The precision of a $\phi_s^{c\bar{c}s\bar{s}}$ measurement in the $f_0(980)$ channel is expected to be poorer than in the ϕ channel because of the smaller decay branching ratio for this process. However, a complementary method of analysis provides different systematic uncertainties, as well as an important cross check of the result from $B_s^0 \to J/\psi\phi$.

In this article, we present a measurement of the relative branching fraction ($R_{f_0/\phi}$) which is, based on theoretical estimates, expected to be significant [7–11]:

$$R_{f_0/\phi} \equiv \frac{\Gamma(B_s^0 \to J/\psi f_0(980), f_0(980) \to \pi^+\pi^-)}{\Gamma(B_s^0 \to J/\psi\phi, \phi \to K^+K^-)} \approx 0.20\text{–}0.40. \quad (1)$$

[*]Visitor from Augustana College, Sioux Falls, SD, USA.
[†]Visitor from The University of Liverpool, Liverpool, UK.
[‡]Visitor from UPIITA-IPN, Mexico City, Mexico.
[§]Visitor from SLAC, Menlo Park, CA, USA.
[‖]Visitor from University College London, London, UK.
[¶]Visitor from Centro de Investigacion en Computacion—IPN, Mexico City, Mexico.
[**]Visitor from ECFM, Universidad Autonoma de Sinaloa, Culiacán, Mexico.
[††]Visitor from Universität Bern, Bern, Switzerland.
[‡‡]Deceased.

The LHCb Collaboration has reported [12] a first measurement of $R_{f_0/\phi} = 0.252^{+0.046}_{-0.032}(\text{stat})^{+0.027}_{-0.033}(\text{syst})$. The Belle Collaboration has measured the branching fraction $\mathcal{B}(B_s^0 \to J/\psi f_0(980),\ f_0(980) \to \pi^+\pi^-) = [1.16^{+0.31}_{-0.19}(\text{stat})^{+0.15}_{-0.17}(\text{syst})^{+0.26}_{-0.18}(N_{B_s^{(*)}\bar{B}_s^{(*)}})] \times 10^{-4}$ [13], where $N_{B_s^{(*)}\bar{B}_s^{(*)}}$ is the number of $B_s^{(*)}\bar{B}_s^{(*)}$ pairs in the sample. The CDF Collaboration has also measured the relative branching fraction and finds $R_{f_0/\phi} = 0.257 \pm 0.020(\text{stat}) \pm 0.014(\text{syst})$ [14]. We report a new measurement of the relative branching fraction using data collected with the D0 detector at the Fermilab Tevatron Collider.

To determine an absolute branching fraction requires an excellent understanding of efficiencies, other related branching fractions, cross sections, and integrated luminosity. However, by measuring a relative branching fraction, terms common to both the $B_s^0 \to J/\psi f_0(980)$ and the $B_s^0 \to J/\psi\phi$ decays cancel, giving:

$$R_{f_0/\phi} = \frac{N_{B_s^0 \to J/\psi f_0(980)}}{N_{B_s^0 \to J/\psi\phi}} \cdot \frac{\varepsilon_{\text{reco}}^{B_s^0 \to J/\psi\phi}}{\varepsilon_{\text{reco}}^{B_s^0 \to J/\psi f_0(980)}}. \tag{2}$$

Hence, just the yields $N_{B_s^0 \to J/\psi f_0(980)}$ and $N_{B_s^0 \to J/\psi\phi}$ and their detection efficiencies, $\varepsilon_{\text{reco}}^{B_s^0 \to J/\psi\phi}$ and $\varepsilon_{\text{reco}}^{B_s^0 \to J/\psi f_0(980)}$, are needed to measure $R_{f_0/\phi}$.

The D0 detector is described in Ref. [15], and only those components that directly affect this measurement are discussed below. The tracking system consists of a silicon microstrip tracker (SMT) and a central fiber tracker (CFT), both located within a 1.9 T superconducting solenoid magnet. The SMT has approximately 800 000 individual strips, with typical pitch of 50–80 μm, and a design optimized for tracking and vertexing capability within the pseudorapidity range $|\eta| < 3$ [16]. The system has a six-barrel longitudinal structure, each barrel having four layers arranged axially around the beam pipe, interspersed with 16 radial disks. The CFT has eight thin coaxial barrels, each supporting two doublets of overlapping scintillating fibers of 0.835 mm diameter. One doublet is parallel to the collision axis, and the others alternate by $\pm 3°$ relative to that axis. The muon system resides beyond a calorimeter that surrounds the inner tracking detectors, and consists of one layer of tracking detectors and scintillation trigger counters before 1.8 T toroids, followed by two similar layers after the toroids.

Approximately 8 fb^{-1} of integrated luminosity is used in this analysis. The data are divided into four time periods, corresponding to different detector configurations and instantaneous luminosities, called Run IIa (1.4 fb^{-1}), Run IIb1 (1.4 fb^{-1}), Run IIb2 (3.3 fb^{-1}), and Run IIb3 (2.1 fb^{-1}).

We search for $B_s^0 \to J/\psi f_0(980)$ candidates using the decay mode $J/\psi \to \mu^+\mu^-$. Events are collected using a mixture of single and dimuon triggers which have a similar trigger efficiency for both $B_s^0 \to J/\psi f_0(980)$ and $B_s^0 \to J/\psi\phi$. Muon candidates must have transverse momentum $p_T > 1.5$ GeV and be detected in the muon chambers within the toroidal magnet. In addition, each muon track must be associated with a track reconstructed by the CFT, and have at least one SMT hit. The J/ψ candidates are formed from two oppositely charged muon candidates emanating from a common vertex, and have at least one of the muon candidates detected outside the toroidal magnet.

All reconstructed tracks not associated with muons forming a J/ψ candidate are considered in the reconstruction of $f_0(980)$ and ϕ candidates. Since the D0 detector has limited ability to separate kaons from pions, tracks are assigned the pion mass when searching for $B_s^0 \to J/\psi f_0(980)$ and the kaon mass when searching for $B_s^0 \to J/\psi\phi$. Charged tracks are required to have at least two CFT hits, at least two SMT hits, a total of at least eight SMT and CFT hits, and a minimum p_T of 300 MeV. Any two oppositely charged tracks that have one track with transverse momentum $p_T > 1.4$ GeV, an invariant mass $0.7\ \text{GeV} < M_{\pi^+\pi^-} < 1.2\ \text{GeV}$ or $1.0\ \text{GeV} < M_{K^+K^-} < 1.05$ GeV, and are consistent with originating from a common vertex, are considered as $f_0(980)$ and ϕ candidates, respectively. The $\mu^+\mu^-\pi^+\pi^-$ ($\mu^+\mu^-K^+K^-$) candidates are required to form a common vertex and have an invariant mass between 5.0 and 5.8 GeV. The invariant mass requirements on $M_{\pi^+\pi^-}$ and $M_{K^+K^-}$ prevent the two tracks to be considered as candidates for both $f_0(980)$ and ϕ interpretations.

The final data sample is formed by applying the following additional requirements to further reduce backgrounds. The $f_0(980)$ and ϕ candidates must have $p_T > 1.6$ GeV with $0.91\ \text{GeV} < M_{\pi^+\pi^-} < 1.05\ \text{GeV}$ and $1.01\ \text{GeV} < M_{K^+K^-} < 1.03$ GeV. The B_s^0 candidates are required to have $p_T > 5$ GeV, $2.9\ \text{GeV} < M_{\mu^+\mu^-} < 3.2$ GeV, and have a proper decay length with a significance of greater than 5 standard deviations (sd).

The proper decay length, defined as $L_{xy} \cdot (M_{B_s^0}/p_T)$, where p_T is the transverse momentum of the B_s^0, $M_{B_s^0}$ is the world average B_s^0 mass [17], and L_{xy} [18] is the transverse distance between the primary $p\bar{p}$ interaction vertex and the four-track vertex of the B_s^0 candidate, is calculated for candidate primary vertices that use the transverse beamspot as a constraint. If there is more than one such vertex in an event, the primary vertex nearest in the transverse plane to the J/ψ candidate is chosen for this analysis.

A final selection is based on two boosted decision tree [19,20] (BDT) discriminants. We use the Monte Carlo simulation (MC) PYTHIA program [21] to generate B_s^0 events and the EVTGEN program [22] to simulate their decay. MC signal and background samples are used to train a BDT and to form discriminant output values for each event. The expected background is primarily due to two sources: prompt background that is defined as directly produced J/ψ mesons accompanied by tracks from

hadronization, and nonprompt, or inclusive $B \to J/\psi + X$ decays where the J/ψ meson arises from a b-hadron decay accompanied by tracks from hadronization. Two MC background samples are therefore generated with PYTHIA: a sample of directly produced J/ψ prompt events and an inclusive sample of B_s^0 for all decay processes $B_s^0 \to J/\psi + X$. A MC signal sample of $J/\psi f_0(980)$ events is used to train both BDTs. Thirty input variables are used in the BDT, including the momenta of final-state objects, vertex-quality requirements, B_s^0 isolation, and the decay angles θ, φ and ψ in the traversity basis [2]. Six isolation variables are used in the BDT representing different choices for the tracks included in the isolation cone and for the size of this cone [23]. The BDT selections for both prompt and inclusive training are defined with a requirement on the BDT output value which provides large $S/\sqrt{B}$, while keeping the signal yields high, where S and B are the number of signal and background events.

The invariant masses of $f_0(980)$ and $B_s \to J/\psi f_0(980)$ candidates, following BDT selections are shown in Figs. 1 and 2, respectively. An unbinned likelihood fit is used to determine the yield of signal in each sample. The $f_0(980)$ has a large width [17] and a mass just below the KK threshold. This affects the line shape, which is not a simple Breit-Wigner form, particularly at large mass values. The $\pi^+\pi^-$ mass distribution is therefore fitted using the functional form of Ref. [24], which takes account of the opening of the KK threshold, and is convoluted with a Gaussian resolution function with a sd of 15 MeV. The line shape determined by fitting the $f_0(980)$ in MC, using a second-degree polynomial for the background, is also used to fit the data. Candidates for $B_s^0 \to J/\psi f_0(980)$ are defined by the $\pi^+\pi^-$ invariant mass window $0.91 < M_{\pi^+\pi^-} < 1.05$ GeV. The $B_s^0 \to J/\psi f_0(980)$ mass distribution is fitted to a Gaussian signal, with a background function consisting of a second-degree polynomial and a Gaussian at lower invariant mass to take into account partially reconstructed B decays. The unbinned likelihood fit is used to determine the contribution to signal in each sample. The $J/\psi f_0(980)$ mass distribution shown in Fig. 2 yields a fitted B_s^0 mass of 5.3748 ± 0.0036 GeV and 590 ± 84 B_s^0 events, where the uncertainties reflect just the statistical uncertainties on the fit.

Using identical event selections, except for the $f_0(980)$ mass requirement, a clear $J/\psi\phi$ peak is found, as shown in Fig. 3. The $\mu^+\mu^-K^+K^-$ mass distribution is fitted for a $B_s^0 \to J/\psi\phi$ signal using a double Gaussian function with a second-order polynomial for background. An unbinned likelihood fit to the $J/\psi\phi$ distribution shown in Fig. 3 yields a B_s^0 mass of 5.3631 ± 0.0008 GeV and 2929 ± 62 B_s^0 events, where again the uncertainties are statistical only.

MC signal samples are used to determine the efficiencies of reconstructing the two B_s^0 decay modes. To take account of changes in the instantaneous luminosity, the MC samples are overlaid with data events from random beam crossings collected during each run period. In the generation of both the $B_s^0 \to J/\psi\phi$ and the $B_s^0 \to J/\psi f_0(980)$ MC signals, a preselection requirement of $p_T > 0.4$ GeV is imposed on both kaons and pions from the ϕ and

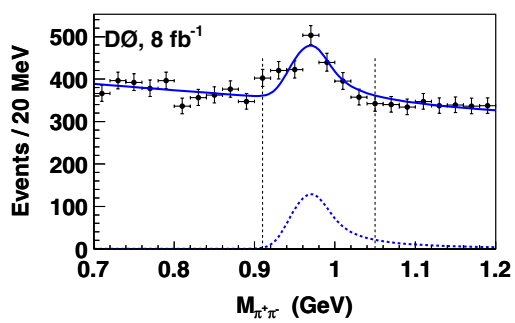

FIG. 1 (color online). The invariant mass distribution of $f_0(980)$ candidates when the $J/\psi\pi^+\pi^-$ invariant mass is within ± 2 sd of the fitted mean B_s^0 mass. The solid line represents the fit to all the data, and the dashed line the fitted $f_0(980)$ signal (see text). The vertical dashed lines indicate the region 0.91 GeV $< M_{\pi^+\pi^-} < 1.05$ GeV.

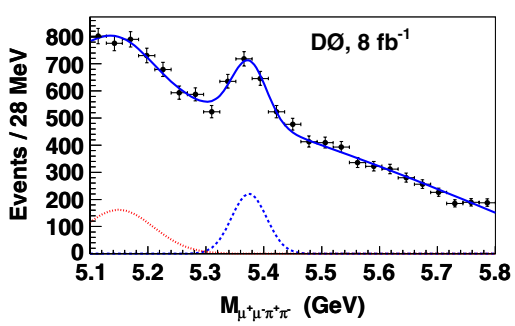

FIG. 2 (color online). The invariant mass distribution of B_s^0 candidates when the $\pi^+\pi^-$ invariant mass is consistent with that of a $f_0(980)$ meson, i.e., $0.91 < M_{\pi^+\pi^-} < 1.05$ GeV. The solid line is the fit to all the data and the dashed line the fitted B_s^0 signal. The dotted line is a Gaussian function used to describe partially reconstructed B decays (see text).

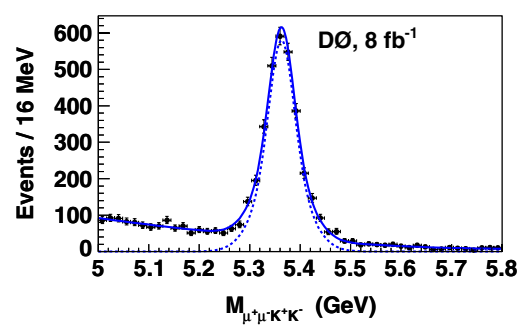

FIG. 3 (color online). The invariant $J/\psi K^+K^-$ mass distribution when the K^+K^- invariant mass is consistent with a ϕ meson, i.e., $1.01 < M_{K^+K^-} < 1.03$ GeV. The solid line is the fit to all the data and the dashed line is the part fitted to B_s^0 signal (see text).

$f_0(980)$. Since the p_T distributions of pions and kaons differ, the preselection efficiencies are determined from two additional MC sets of events generated without p_T cutoffs.

Reconstruction efficiencies depend on the data-taking period (Run IIa–IIb3) as instantaneous luminosity, aging of the detector, and changes to the reconstruction algorithms affect detector performance. The reconstruction efficiencies are therefore measured separately for each running period. The instantaneous luminosities for data taken during Run IIb3 are similar to those of Run IIb2, and the reconstruction efficiencies for Run IIb2 are therefore also used for Run IIb3 data. Although the absolute reconstruction efficiencies depend on the running period, the relative reconstruction efficiencies given in Table I are stable. The differences in relative reconstruction efficiency are used to estimate a systematic uncertainty on $R_{f_0/\phi}$. The mean relative reconstruction efficiency is 1.20 ± 0.04, where the uncertainty is from statistics in the MC.

The $B_s^0 \to J/\psi\phi$ time development reflects a mix of two exponential functions with relative slope values driven by the difference in decay widths of the two mass eigenstates ($\Delta\Gamma_s$). The relative efficiency of any cutoff on proper decay length for the two states depends on $\Delta\Gamma_s$ and the lifetime of the CP-odd eigenstate. The MC samples used to determine the relative efficiency use $\Delta\Gamma_s = 0$ and the world average Γ_s value [17]. For this $\Delta\Gamma_s$, and assuming no CP violation, the effect on the relative efficiency of $f_0(980)/\phi$ is found to be small ($\approx 2.5\%$) and well within systematic uncertainties, and therefore no correction is applied.

The branching fraction of $B_s^0 \to J/\psi f_0(980)$ is measured relative to $B_s^0 \to J/\psi\phi$, so any backgrounds that peak under the $B_s^0 \to J/\psi\phi$ mass distribution will affect the measurement of $R_{f_0/\phi}$. Possible $\mathcal{S}$-wave contributions can arise from the f_0 or from nonresonant K^+K^- production, but these contributions provide only slowly varying contributions under the ϕ mass peak. The excess for larger $M_{K^+K^-}$ is extrapolated under the ϕ mass, giving a possible $\mathcal{S}$-wave contribution of $(12 \pm 3)\%$ [25] of the total $B_s^0 \to J/\psi\phi$ yield. The relative branching ratio is therefore scaled up by a factor of $1/0.88$ to account for an $\mathcal{S}$-wave contribution to $B_s^0 \to J/\psi\phi$.

One possible background that can affect the observed $B_s^0 \to J/\psi f_0(980)$ yield is the three-body decay $B_s^0 \to J/\psi\pi^+\pi^-$. This background is studied by measuring the B_s^0 yield for $\pi^+\pi^-$ invariant masses less than the $f_0(980)$ mass. The $\pi^+\pi^-$ mass distribution from nonresonant $B_s^0 \to J/\psi\pi^+\pi^-$ is broad, and measuring the B_s^0 yield for a sideband in $M_{\pi^+\pi^-}$ therefore provides an extrapolation of the nonresonant $\pi^+\pi^-$ background to the $f_0(980)$ signal region. In defining a $\pi^+\pi^-$ mass window to study this background, it is important to avoid regions where other known resonances, e.g., $B_s^0 \to J/\psi K^*$, $K^* \to K\pi$ (with the kaon assigned the pion mass) can contribute. The $\pi^+\pi^-$ mass window of 0.8–0.9 GeV is chosen because this mass range has no overlap with $B_s^0 \to J/\psi K^*$ events.

The mass distribution of $\mu^+\mu^-\pi^+\pi^-$, for $0.8 < M_{\pi^+\pi^-} < 0.9$ GeV, is fitted with a floating contribution from nonresonant $J/\psi\pi^+\pi^-$ decays. The mean and the width of the B_s^0 peak are constrained to the values obtained from the corresponding fit in the $f_0(980)$ signal region. The fit yields 42 ± 49 events, indicating no evidence of $B_s^0 \to J/\psi\pi^+\pi^-$ nonresonant background, and consequently no such correction is used in this analysis.

To check that the results of the analysis do not depend on the specific choice of the selection critera, each cut is changed around its nominal value, and it is observed that $R_{f_0/\phi}$ does not depend significantly on the exact choice of selections.

The large backgrounds arising from particle combinatorics and from partially reconstructed B decays provide significant distortion and uncertainties in the distributions of background. We study this using same-charge pions and the mass distribution from $\mu^+\mu^-\pi^\pm\pi^\pm$ events. However, we find that the $\mu^+\mu^-\pi^\pm\pi^\pm$ distribution does not describe the measured background in our signal sample and we therefore do not use it to help constrain the distribution of the background. Instead, different parametrizations are used (third-degree polynomial and an exponential) to describe the background, and different mass regions over which the fit is performed are used to determine the signal yield variation. A large variation in the number of signal events for $B_s^0 \to J/\psi f_0(980)$ is found for different parametrizations of the background, indicating that modeling of the background has substantial ambiguity. The choice of background parametrization comprises the largest contribution to the total systematic uncertainty on $R_{f_0/\phi}$.

A similar study of fitting choices is performed on the $B_s^0 \to J/\psi\phi$ sample. However, since these backgrounds are much smaller and easier to describe, the measured event yields change by less than 1%. The presence of a $B^0 \to J/\psi\pi^+\pi^-$ contribution is checked by including this channel in the fit, yielding a fit consistent with no events.

The MC distributions of the kinematic variables do not describe the data perfectly in all variables. To study this effect on the training of the BDT, the MC signal distributions used to train the BDT are weighted to match the $B_s^0 \to J/\psi\phi$ data. A weighting of $B_s^0 \to J/\psi\phi$ signal BDT distributions is used to better match the overall $B_s^0 \to J/\psi\phi$ data, and these weights were applied to both MC signal distributions. Only the $B_s^0 \to J/\psi\phi$ events are used for this

TABLE I. Relative reconstruction efficiencies for different running periods.

Run period	$\varepsilon_{\rm reco}^{B_s^0\to J/\psi\phi}/\varepsilon_{\rm reco}^{B_s^0\to J/\psi f_0(980)}$
Run IIa	1.19 ± 0.03
Run IIb1	1.29 ± 0.04
Run IIb2 + IIb3	1.20 ± 0.05

TABLE II. Systematic uncertainties in the branching fraction ratio, $R_{f_0/\phi}$.

Source	Uncertainty
Fitting	17.3%
MC efficiency	9.2%
Modeling variables in BDT	8.9%
$f_0(980)$ mass window	4.0%
$\mathcal{S}$-wave contribution	3.5%
Total	22.2%

purpose because in the $B_s^0 \to J/\psi f_0(980)$ channel there is much background and a far smaller signal fraction.

Using the Run IIb2 data and Run IIb2 MC, we find that the relative efficiency for event reconstruction changes from 1.20 ± 0.04 without reweighting to 2.00 ± 0.07 after weighting. Although this corresponds to a large difference in relative efficiency, the relative yields also change, thereby changing $R_{f_0/\phi}$ by just 17.8%. Half of the difference between the nominal result and the reweighted BDT result is taken as a systematic uncertainty on $R_{f_0/\phi}$. A 4.0% systematic uncertainty is assigned for the observed dependence of $R_{f_0/\phi}$ on the size of the $f_0(980)$ mass window. Table II summarizes the values of the systematic uncertainties on $R_{f_0/\phi}$.

Based on 8 fb^{-1} of data, D0 has extracted a measurement of the relative branching fraction $R_{f_0/\phi}$ of Eq. (1).

$$R_{f_0/\phi} = 0.275 \pm 0.041(\mathrm{stat}) \pm 0.061(\mathrm{syst}).$$

This agrees with theoretical expectations and with previous measurements of the ratio of widths.

We thank the staffs at Fermilab and collaborating institutions, and acknowledge support from the DOE and NSF (USA); CEA and CNRS/IN2P3 (France); FASI, Rosatom and RFBR (Russia); CNPq, FAPERJ, FAPESP and FUNDUNESP (Brazil); DAE and DST (India); Colciencias (Colombia); CONACyT (Mexico); KRF and KOSEF (Korea); CONICET and UBACyT (Argentina); FOM (The Netherlands); STFC and the Royal Society (United Kingdom); MSMT and GACR (Czech Republic); CRC Program and NSERC (Canada); BMBF and DFG (Germany); SFI (Ireland); The Swedish Research Council (Sweden); and CAS and CNSF (China).

[1] V. M. Abazov *et al.* (D0 Collaboration), Phys. Rev. Lett. **101**, 241801 (2008).
[2] V. M. Abazov *et al.* (D0 Collaboration), arXiv:1109.3166 [PRD (to be published)].
[3] T. Aaltonen *et al.* (CDF Collaboration), Phys. Rev. Lett. **100**, 161802 (2008).
[4] A. Lenz and U. Nierste, J. High Energy Phys. 06 (2007) 072.
[5] R. Fleischer, R. Knegjens, and G. Ricciardi, Eur. Phys. J. C **71**, 1832 (2011).
[6] I. Dunietz, R. Fleischer, and U. Nierste, Phys. Rev. D **63**, 114015 (2001).
[7] S. Stone and L. Zhang, arXiv:0909.5442.
[8] S. Stone and L. Zhang, Phys. Rev. D **79**, 074024 (2009).
[9] P. Colangelo, F. De Fazio, and W. Wang, Phys. Rev. D **81**, 074001 (2010); Phys. Rev. D **83**, 094027 (2011).
[10] O. Leitner, J.-P. Dedonder, B. Loiseau, and B. El-Bennich, Phys. Rev. D **82**, 076006 (2010).
[11] K. M. Eckland *et al.* (CLEO Collaboration), Phys. Rev. D **80**, 052009 (2009).
[12] R. Aaij *et al.* (LHCb Collaboration), Phys. Lett. B **698**, 115 (2011).
[13] J. Li *et al.*, Phys. Rev. Lett. **106**, 121802 (2011).
[14] T. Aaltonen *et al.* (CDF Collaboration), Phys. Rev. D **84**, 052012 (2011).
[15] V. M. Abazov *et al.* (D0 Collaboration), Nucl. Instrum. Methods Phys. Res., Sect. A **565**, 463 (2006).
[16] Pseudorapidity is defined as $\eta = -\ln[\tan(\theta/2)]$, where θ is the polar angle relative to the proton-beam direction.
[17] K. Nakamura *et al.* (Particle Data Group), J. Phys. G **37**, 075021 (2010).
[18] D0 uses a right handed coordinate system with the z-axis pointing along the axis of the proton beam.
[19] L. Breiman *et al.*, *Classification and Regression Trees* (Wadsworth, Stamford, 1984).
[20] A. Höcker *et al.*, Proc. Sci., ACAT (2007) 040.
[21] T. Sjöstrand *et al.*, Comput. Phys. Commun. **135**, 238 (2001).
[22] D. J. Lange, Nucl. Instrum. Methods Phys. Res., Sect. A **462**, 152 (2001).
[23] See Appendix A in Ref. [2].
[24] J. B. Gay *et al.*, Phys. Lett. B **63**, 220 (1976); S. M. Flatté, Phys. Lett. B **63**, 224 (1976); Phys. Lett. B **63**, 228 (1976).
[25] See Appendix B in Ref. [2].